An Equilibrium Ablation Boundary Condition for the Data-Parallel Line-Relaxation Code

Matthew MacLean[1]
CUBRC, Buffalo, NY, 14221

A Gibbs free-energy minimization solver has been developed to compute the equilibrium saturated mixture composition and blowing rate for complex gas/thermal protection system combinations where the surface acts as a source of multiple constituents. This tool has been embedded in the Data-Parallel Line-Relaxation computational fluid dynamics code to perform simulations with equilibrium ablation in a tightly-coupled manner. Such an implementation eliminates the need for blowing corrections for material response analysis.

Nomenclature

B'	=	dimensionless blowing rate
C_H	=	heat transfer coefficient
c	=	mass fraction of gaseous species
G_i	=	chemical potential of species i
J	=	diffusion flux
$\dot{m}$	=	mass blowing rate
M	=	molecular weight
P	=	pressure
$\bar{R}$	=	universal gas constant
T	=	temperature
U	=	freestream velocity
β	=	mass fraction of bulk species
ε	=	emissivity
η_i	=	mole-mass ratio of species i
η	=	total gaseous mole-mass ratio
λ	=	empirical blowing parameter
Λ	=	Lagrangian variable
ρ	=	density
ψ	=	elemental stoichiometric factor

I. Introduction

THE coupling of the effects of ablation chemistry to the gaseous flowfield within the shock layer of a reentry body has been a subject of a number of recent studies[1-8]. The approaches taken vary considerably depending on the particular application of interest and the codes that are employed to model the gasdynamic flowfield and the thermal protection system (TPS) response. To a large extent, the details of the approach are driven by the timescales of the material response process – for leading edges or nosetips where heating rates are extremely high, and recession and shape change are correspondingly rapid, a tightly coupled approach where the gaseous flowfield and the material response are iterated simultaneously with actively recessing boundary conditions implemented at the gas/surface interface should be taken. Such an approach has been taken with success, for example, by Martin and Boyd[1] and Nompelis, et al.[2]

For a second class of applications where the material response process occurs on a timescale that is significantly longer than the changing fluid motion, efficient solution may be obtained with less expense than coupling both simulations so tightly together. Such cases often occurs with planetary reentry capsules which enter the atmosphere at low density with high speed and descend through the atmosphere with a fairly low heat rate per unit area. In this

[1] Senior Research Scientist.

application, instantaneous shape change is usually not considered because of the disperate timescales involved and the large radius of curvature to recession length scale; however, the importance of the interaction of gaseous and ablation chemistry is still relevant because the effect of the ablation chemistry in the near-surface region can significantly affect the nature of the gaseous boundary layer and, hence, the heating rate to the surface.

Traditionally, in many cases, this class of problems was solved using an uncoupled approach, where the heat and/or mass transfer rates were extracted from a non-ablating computational fluid dynamics (CFD) solution and applied as boundary conditions to a separate material response code[3]. This process is conceptually shown in Fig. 1(a). Using an uncoupled approach, the effects of the release of the ablation products into the gaseous flowfield and the accompanying surface blowing that occurs is not accounted for in the baseline CFD solution. Instead, a common approximation is to employ a "blowing correction" based on boundary-layer theory that is given in Eq. (1), where $C_{H,0}$ is the non-blowing (baseline) heat transfer coefficient from the CFD solution and B_0' is the corresponding dimensionless mass flux ratio as defined in Eq. (2), which can be found using $C_{H,0}$ by assuming that $C_M = C_H$ with unity Prandtl/Lewis numbers and equal species diffusion. In Eq. (1), the parameter λ appears, which has a traditional value of 0.5 but can be used empirically to adjust the blowing correction to match experimental data or expected output.

$$\frac{C_H}{C_{H,0}} = \frac{2\lambda B_0'}{e^{2\lambda B_0'} - 1} \tag{1}$$

$$B' = \frac{\dot{m}}{\rho_e U_e C_M} \approx \frac{\dot{m}}{\rho_e U_e C_H} \tag{2}$$

A better practice would generally be to take the output from the material response code back as a direct boundary condition for a second iteration of the CFD flowfield and continue to iterate between the two codes until a convergent solution is obtained. This would eliminate the need to use Eqn. (1). Such a thing has sometimes been done, for example by Olynick, et al.[4], who found that about three iterations were required between their CFD and material response codes before the heat flux through the surface interface was banded within 5%. This approach may be considered a loosely coupled approach since it eliminates the need for the approximation of Eqn. (1) but retains Eqn. (2) to determine surface response.

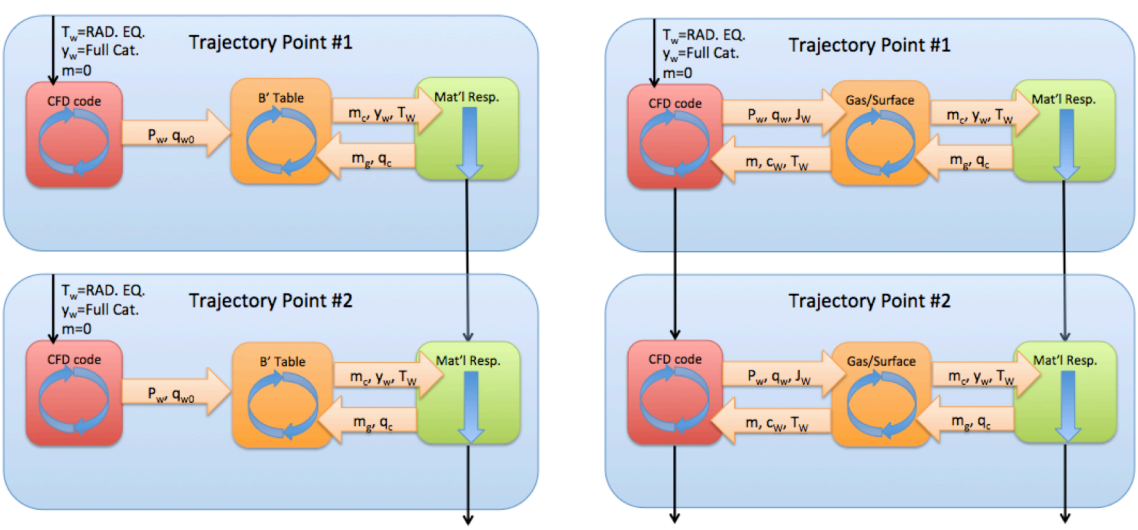

(a) Uncoupled Approach (b) Tightly Coupled Approach

Figure 1. Flow Charts Describing CFD/Material Response Coupling Processes

Since the surface boundary mass fluxes are computed within the CFD solver as part of the solution, the best practice would be to provide the mass fluxes directly as input to the material response analysis rather than the heat flux, and reliance on the mass transfer analogy implied by Eqn. (2). This approach also requires the CFD and the material response solutions to be iteratively converged to a consistent state as shown schematically in Fig. 1(b).

Johnston, et al.[5] investigated these two approximations in detail and demonstrated that their use can drastically alter the predicted blowing rate under certain circumstances, particularly when the flow is turbulent.

A recent parallel approach incorporated finite-rate surface chemistry via a generalized set of physical mechanisms including limited aspects of pyrolysis and steady-state energy balance conduction[6-7]. This model was coupled implicitly into the CFD solver such that it was converged each iteration with the CFD flowfield and provided real-time Jacobian information to the implicit linear system. Such a model incorporates a great deal of physics of the gas/surface interaction process, but it requires accurately knowing a significant number of parameters and physical insight about the dominant mechanisms at the surface. For systems where the physical reaction mechanisms are close to equilibrium, an equilibrium formulation is far simpler and requires far fewer parameters.

In this work, an approach is taken that is similar to Johnston, et al.[5] and Bianchi, et al.[8] to tightly couple the effect of ablation product addition to the gaseous boundary layer by implementing equilibrium ablation surface chemistry. Here, a solver to compute the equilibrium composition and mass addition of saturated gas/bulk mixtures has been connected to the CFD simulation to provide boundary condition information that satisfies surface mass and energy balances. The broad goal of this effort has been to take a first step toward coupling the CFD solver to an arbitrary material response code that computes the detailed in depth conduction, material breakdown, and sub-surface response of the TPS material using the accurate exchange of information implied by Fig. 1(b). Therefore, the saturated equilibrium mixture solver has been constructed as a "black-box" algorithm to the CFD code to mimic the incorporation of a material response code for which detailed internal solver information is not available or not convenient to obtain in order to better understand the difficulties in tightly coupling two codes together without the exchange of high-order Jacobian information. A secondary benefit to this effort is that that use of the equilibrium mixture solver can potentially provide a realistic CFD solution to use as a first guess to transmit to the interfacing and material response code (one can presume it must at least be a better first guess than the non-blowing, gas-only solution…).

II. Equilibrium Saturated Mixture Solver

The equilibrium solver performs a Gibbs free energy minimization for a fixed value of temperature and pressure closely following the implementation of Gordon and McBride[9] that was developed and refined for the community-standard Chemical Equilibrium with Applications (CEA) code. The equilibrium composition of a mixture of gaseous species and condensed species is computed subject to an additional number of elemental constraints, which are incorporated using Lagrange multiplier degrees of freedom.

For gaseous species, the minimization of the Gibbs energy of the system is expressed through a series of dimensionless chemical potential equations with elemental constraints, defined as in Eqn. (2).

$$\frac{G_i^0}{\bar{R}T} + \ln(\eta_i) - \ln(\eta) + \ln\left(\frac{P}{P_{REF}}\right) - \sum_{k=1}^{Ne} \psi_{k,i}\Lambda_k = 0 \tag{2}$$

For condensed species, the constrained chemical potential equation is defined in Eqn. (3).

$$\frac{G_j^0}{\bar{R}T} - \sum_{k=1}^{Ne} \psi_{k,j}\Lambda_k = 0 \tag{3}$$

The system is closed with Ne elemental balance constraints and a total mass constraint given in Eqns. (4) and (5).

$$\sum_{i=1}^{Ng} \psi_{k,i}\eta_i + \sum_{j=1}^{Nb} \psi_{k,j}\eta_j = \sum_{i=1}^{Ng} \psi_{k,i}\tilde{\eta}_i + \sum_{j=1}^{Nb} \psi_{k,j}\tilde{\eta}_j = \tilde{b}_k^0 \tag{4}$$

$$\sum_{i=1}^{Ng} \psi_{k,i}\eta_i = \eta \tag{5}$$

In Eqns. (2) – (5), the amount of each chemical species is most naturally expressed with a mole/mass ratio, η_i (number of moles of species *i* per unit mass of mixture). With care, other measures of amount such as concentration can be utilized in a generic free-energy minimization system[6], but here, the algorithm used by CEA is followed as precisely as possible. This system is solved iteratively using a Newton-Raphson technique, with details given by Gordon and McBride for the CEA code. As noted by Blackwell and Howard[11], solution of this system is equivalent to the minimization of a composite Lagrangian function inclusive of the Lagrange multipliers (Λ_k) treated as independent variables.

A major advantage of the Gordon and McBride approach is that the gas phase composition variables (η_i) appear in an isolatable way in the equation set and can be eliminated from the solution in order to greatly reduce the size of the resulting linear system. Via their procedure, the system given by Eqns. (2) – (5) consisting of $N_g+N_b+N_e+1$ equations can be significantly reduced to N_b+N_e+1 by substituting Eqn. (2) into the others. The reduced linear system is iteratively solved using Newton-Raphson, and then the gas phase composition can be found from Eqn. (2) as a post-processing step. In this way, there is virtually no penalty to the inclusion of a large number of gaseous species into the system. In this particular application, inclusion of gaseous species is clearly limited by the CFD code, which must solve a transport equation for each of those species included.

The details of the solution procedure are comprehensively described by Gordon and McBride, so they are not repeated here, except to say that the system can be highly unstable with the addition of condensed species, so it was found that the solution limiting proposed by those authors had to be followed very closely to insure convergence. This includes treating the actual independent variables as the natural logs of the mole mass ratios to help avoid negative values as well as the limiting employed during each Newton-Raphson update.

Further, as part of their implementation, the free energy of the system is first solved with gas phase species only. Then, a test is performed to determine if the presence of any of the condensed phase species can further reduce the free-energy in the system and, if so, which one is determined to reduce it the most. This test is performed by evaluating Eqn. (6). The CEA database[10] includes data for both solid and liquid phase states for many species. In this effort, no attempt is made to distinguish between condensation to solid or liquid phase, only that the state of the condensate is not gaseous for the purpose of equilibrium gaseous saturation. Tracking of melting or failing liquid flow of the material could easily be incorporated into the code output since no additional work needs to be done to the basic solver algorithm.

$$\frac{G_j^0}{\bar{R}T} - \sum_{k=1}^{Ne} \psi_{k,j}\Lambda_k < 0 \tag{6}$$

Condensed species are added to the system one at a time until the free energy of the system can no longer be reduced. Again, per the Gordon and McBride recipe, any condensed species found to be negative after an update is removed from consideration for the next iteration. In addition, the appearance of certain singularities must be censored, such as when one condensed species is a linear combination of two others. Instances of both of these were observed to arise in considering a C(b)-Si(b)-SiC(b) system below. These three condensed states cannot simultaneously be included in the linear system; at certain temperatures, the condensation test in Eqn. (6) predicts the addition of C(b), then Si(b), then SiC(b), at which point, Si(b) must be removed to determine the final minimized system state.

To obtain the equilibrium saturated mixture state for a selected mix of gas and condensed species, bulk mass is added to the unit mass gaseous system until some of it starts to condense out as any non-gaseous species, triggering addition of one or more condensed species to the equilibrium system. Bulk mass is added one order of magnitude at a time to optimize numerical sensitivity up to a bulk/gas ratio of $1\text{x}10^6$ (which was considered sufficient to make the originating gaseous mass insignificant). The normalized gaseous composition in this system represents the saturated equilibrium mixture of that gas/bulk system. Candler[12] shows that the mass added to saturate the mixture is equivalent to the B' blowing parameter commonly employed in the uncoupled approach, which can be defined in this scenario by Eqn. (7). The algorithm can therefore be used to generate B' tables as well as to provide on-the-fly equilibrium calculations to the coupled CFD code without needing to make the approximations discussed earlier.

$$B' = \frac{c_b}{c_{GAS}} = \left(1 + m_{ADDED}\right)\left(1 - c_{CONDENSED}\right) - 1 \tag{7}$$

A. Elemental Carbon System

For example, consider the mixture of carbon bulk material saturating reacting air. The familiar B' curve for this system can be generated as a function of temperature for different levels of pressure using the above procedure. The equilibrium saturate mixture composition and blowing rate, B', are given in Fig. 1(a) as a function of temperature at a pressure of 30 kPa (0.3 bar). As expected, the equilibrium solver predicts primarily CO oxidation at moderate temperatures and C_3 sublimation followed by C atom sublimation at higher temperatures. Blowing parameter curves for a number of pressures are shown in Fig. 1(b), which exactly match the results published by Candler[12] (Figure 1 in the referenced paper).

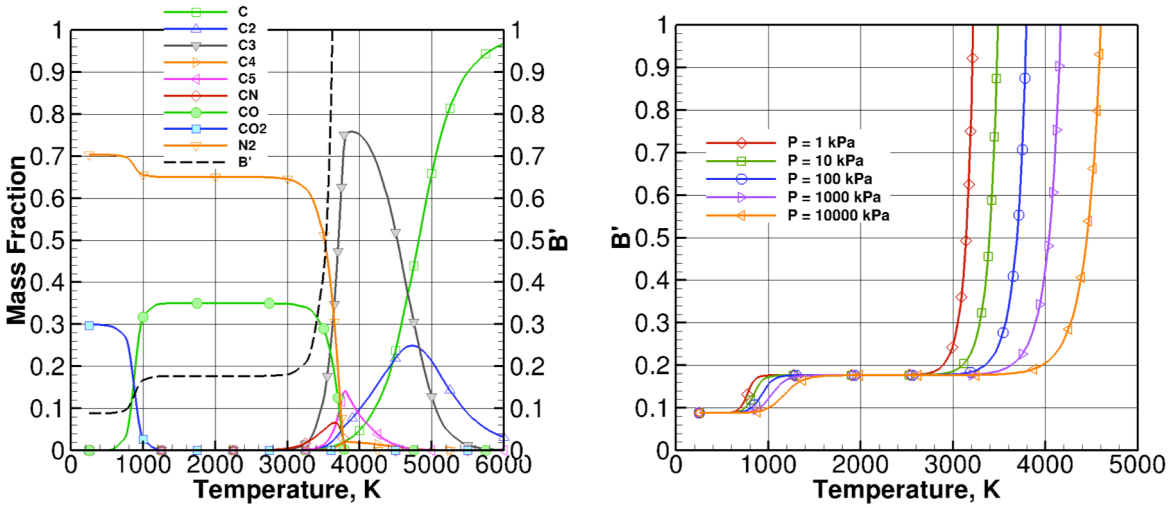

(a) Mass Fractions and B' for Carbon Ablation at 30 kPa

(b) B' for Carbon Ablators at Various Pressures

Figure 1. Equilibrium Saturated Mixture Composition and Dimensionless Blowing Rate for Elemental Carbon Ablator Systems

B. Elemental Silicon System

An advantage of the free-energy minimization approach taken by Gordon and McBride is that multiple condensed species can be present as long as each contributes to reduction of the free energy of the system. A more complex system consisting of multiple bulk elements is also relevant to the modern thermal protection system community. For example, consider the AVCOAT material used on the Apollo missions which is of interest for the upcoming Orion thermal protection system design. According to Graves and Witte[13], AVCOAT char is composed of an approximately equal proportion of carbon and silica, and, thus, provides a source of both elemental carbon and silicon to the equilibrated system.

The equilibrium saturated ablation curve of elemental silicon alone is first considered as shown in Fig. 2(a). Oxidation of silicon forms primarily gaseous SiO at moderate temperatures, followed by Si atom sublimation at higher temperatures. The blowing parameter, B' is higher for silicon oxidation than carbon oxidation because of the increased molecular weight of silicon. Another interesting scenario is the addition of SiO_2(b) as a condensed species product to the silicon system considered above Si(b)-SiO_2(b). Including SiO_2(b) as a condensed species product insures oxygen will consume any available Si bulk and the blowing rate curve at temperatures below about 1000K is actually negative (meaning mass is condensing onto the surface as SiO_2(b)) as shown in Fig. 2(b).

C. Elemental Carbon/Silicon System

One conventional approach to the calculation of equilibrium saturated mixture compositions is to limit the saturation to only a single bulk constituent at a time[14]. Recently, there have been some efforts to incorporate the effects of multiple constituents such as the work of Milos and Marschall[15] or, very recently, Blackwell and Howard[11]. As a fundamental exercise in the spirit of the modeling of AVCOAT char and to test the capabilities of the new solver to produce a solution with two bulk elemental constituents, the scenario of combined carbon and silicon equilibrium saturation is considered.

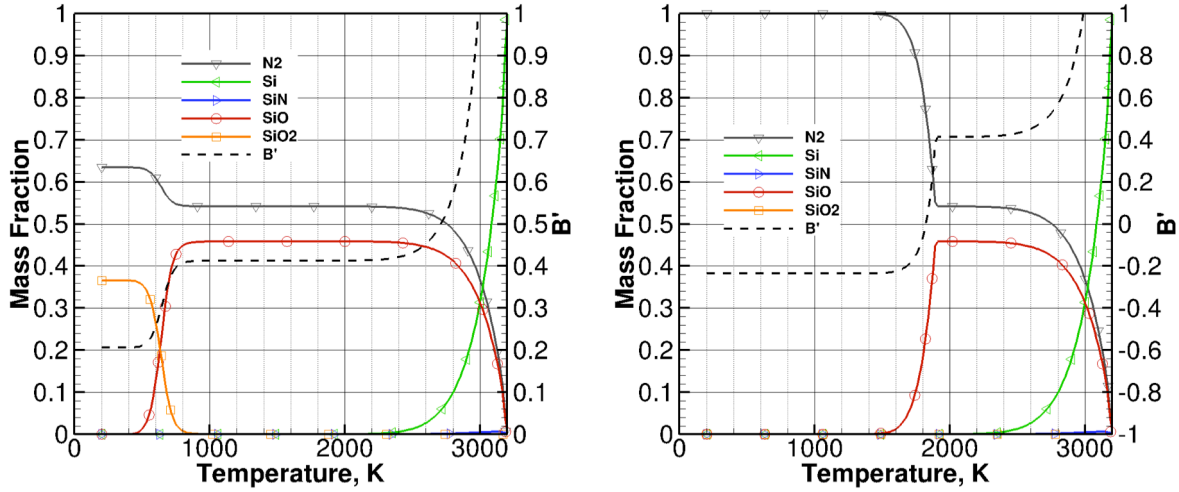

(a) Mass Fractions and B' for Pure Silicon Ablation at 30 kPa

(b) Mass Fractions and B' for Pure Silicon Ablation at 30 kPa with SiO_2(b) Condensation

Figure 2. Equilibrium Saturated Mixture Composition and Dimensionless Blowing Rate for Elemental Silicon Ablator Systems

For a complex bulk system which is assumed to be composed elementally of both carbon and silicon, a significantly more complex behavior occurs. To demonstrate, the bulk system was arbitrarily assumed in this case to be composed of 50% elemental carbon and 50% elemental silicon by mass. The first issue to consider is what is meant by ablation of a surface that is composed of two distinct constituents. After some consideration, the author suggests that ablation of a multiple element bulk is only meaningful if the gas is saturated in the stoichiometric composition of the bulk material. In other words, if (hypothetically) only Material A was contributing to saturating the equilibrium composition of the gas and Material B played no role, then the near surface would, over time, be found to be composed of Material B only with Material A exhausted at the surface and existing only within the depth of the material. Without further considering the in-depth behavior of the material in more detail, we therefore restrict the saturation of the gaseous mixture to be allowed to proceed only by adding bulk material in its stoichiometric ratio (in this case, $\dot{m}_{b,carbon} = 0.5\dot{m}_{b,total}$ and $\dot{m}_{b,silicon} = 0.5\dot{m}_{b,total}$). Bulk mass is added in this ratio until some condensation occurs. The same argument is made by Milos and Chen[16] in their generalization of the Multicomponent Ablation Thermochemistry(MAT) code, which lends some credibility to this implementation.

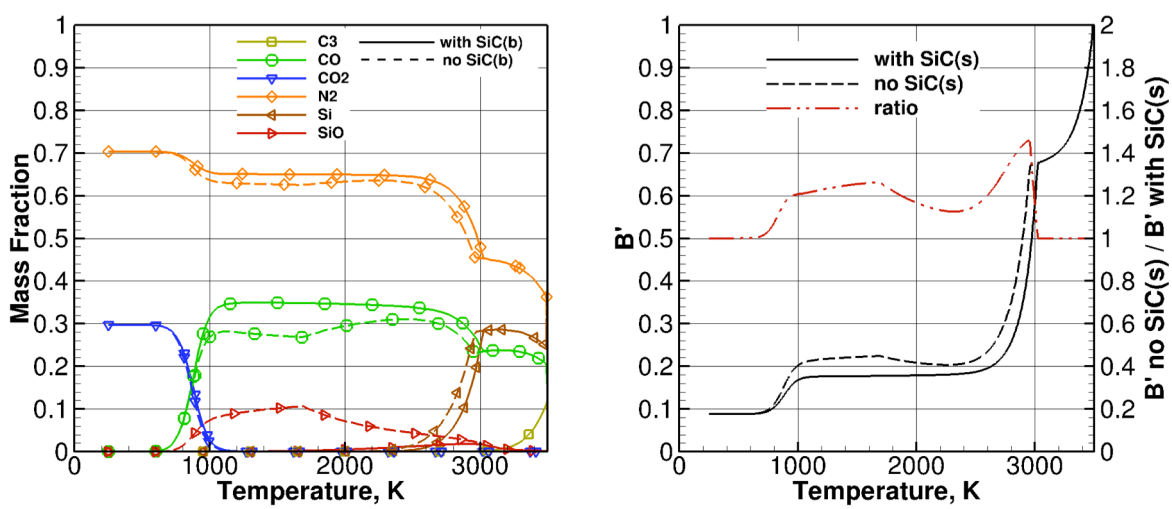

(a) Mass Fraction Comparison

(b) B' Comparison

Figure 3. Equilibrium Saturated Mixture Composition and Dimensionless Blowing Rate for Combined Carbon/Silicon Ablator System at 30kPa

Clearly, when in-depth material response is considered, the situation is not necessarily this simple (with pyrolysis gas motion or porosity allowing access to in-depth gas/surface interaction for example), but this assumption can be justified more easily since the goal of this integration is to obtain a more physically reasonable gaseous solution for iterative material response coupling (where an in-depth material response model could, in principle, supply better boundary conditions on subsequent iterations).

For this system, it was discovered in the solution process that the B' curve is sensitive to the presence of a third condensed element, SiC(b). Essentially, free-energy is minimized most effectively by some of the silicon and carbon mass condensing out as SiC rather than the elemental bulk constituents. This is shown in Fig. 3, which plots the mass fractions of gas species as a function of surface temperature and the blowing rate B' for both systems (Si(b)/C(b) and Si(b)/C(b)/SiC(b)). The blowing rate in Fig. 3(b) also plots the ratio of the two B' values obtained in the two solutions. The increase in blowing mass without the presence of SiC(b) is evident by the partial formation of SiO rather than CO in the oxidation regime (resulting in greater unit mass addition for the available oxygen in the system). Thus we can observe that the blowing rate is sensitive to which condensed species are considered in the solution of the equilibrium system. As with the isolated single element systems, CO and SiO are the important gas phase oxidation products at intermediate temperature ranges with sublimation of Si and eventually C_3 occurring at higher temperatures.

This complex test case does demonstrate that the equilibrium saturated mixture solution only imposes the minimization of free-energy on the system. It does not consider rate mechanics or process feasibility. A well-known example is the formation of CO_2 at low temperatures for the carbon/air system shown in Fig. 1. Pure equilibrium considerations suggest that a carbon heat shield cannot exist in air at room temperature, but the slow formation rate of CO_2 at such a condition precludes instant vaporization. More complex scenarios like the formation of SiC(b) observed above must be evaluated by the user on the basis of knowledge of the material in use. The successful objective of this work was to develop the numerical tool that is capable of solving the equilibrium systems in a generalized way.

D. AVCOAT-like System

Finally, a system is considered composed of 50% bulk carbon (C(b)) and 50% bulk silica (SiO_2(b)) by mass similar to what was prescribed for AVCOAT char by Graves and Witte[13]. For this case, allowed condensed species include C(b), Si(b), SiC(b), and SiO2(b). The resulting gaseous mass fractions and B' are plotted in Fig. 4 as a function of surface temperature at a pressure of 30 kPa. Clearly, the blowing B' curve is much more complex than observed for the earlier pure carbon or pure silicon systems and is composed of a number of distinct zones. At low temperatures, the system behaves as a carbon system, oxidizing to CO_2 (non-physical) at low temperatures and oxidizing as CO at moderate temperatures. At sufficient temperature to liberate SiO_2(b) from the bulk matter, the surface essentially acts as a secondary oxygen resource to increase the fraction of CO with Si(b) remaining as a condensate. At even sufficiently higher temperatures, sublimation occurs of Si followed by C_3, but the sublimation of Si necessarily results in the release of additional oxygen to the gas, resulting in a mixed blowing rate governed by both sublimation and by oxidation simultaneously since the mass fraction of CO remains high.

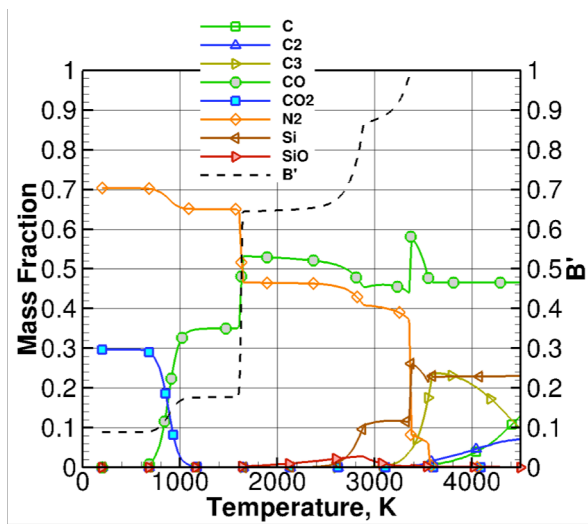

Figure 4. Equilibrium Saturated Mixture Composition and Dimensionless Blowing Rate for C/SiO_2 Ablator Systems at 30 kPa

III. CFD Boundary Condition and Implementation

The equilibrium saturated mixture code described in the previous section constitutes a stand-alone code which may be utilized to generate the B' curves for various gas/bulk systems as shown. In the tightly coupled approach, the B' curve is not required and the boundary conditions at the gas/surface interface in the CFD code can be solved efficiently using the equilibrium solver in real time by embedding the equilibrium saturated mixture routines into the

CFD code binary. For each gas/surface cell face at the boundary of the CFD grid, the surface temperature, pressure, and existing composition are used as input variables. The result of the subroutine call is a new composition (e.g. mass fractions of all gaseous species) which is saturated with as much of the bulk composition as possible. The new mass fractions are set as explicit boundary conditions without implicit coupling to the Jacobian. Implicit coupling requires knowledge of the derivatives of the equilibrium composition fractions with respect to flow variables, either numerically or analytically obtained. This is possible with the saturated equilibrium mixture solver, but one goal of this work was to generate the framework necessary for other material response models, which might come in the form of B' curves or externally linked codes for which the source code or algorithm details are not readily available. For the general case, we simply ignore the implicit contribution of the change in mass fractions and make calls to the saturated equilibrium mixture subroutine at regular, user-specified intervals rather than every iteration. This improves stability for flows where the surface pressure and/or temperature are changing rapidly (e.g. radiative equilibrium walls).

To obtain the mass added to the gaseous system, elemental mass balance is computed for each element contained within the gaseous system, as in Eqn (6).

$$-\sum_{i=1}^{Ng}\left(\frac{\psi_{k,i}M_k}{M_i}\right)J_{i,w}+\dot{m}\sum_{i=1}^{Ng}\left(\frac{\psi_{k,i}M_k}{M_i}\right)c_{i,w}=\dot{m}\sum_{j=1}^{Nb}\left(\frac{\psi_{k,j}M_k}{M_j}\right)\beta_j \qquad [k = 1,N_e] \tag{6}$$

In Eqn. (6), "i" indicates a summation over all gaseous species, N_g, "j" indicates a summation over all bulk species, N_b, and "k" indicates a particular element. Here, $J_{i,w}$ is the diffusive flux of each species to the surface, $c_{i,w}$ is the gaseous mass fraction of that species at the wall, and β_j is the mass fraction of a particular species in the bulk. More compactly, Eqn (6) may be written as:

$$-J_{k,w}+\dot{m}c_{k,w}=\dot{m}\beta_k \qquad [k = 1,N_e] \tag{7}$$

The elemental mass balance constraint balance the diffusive flux and the convection of each element into the gas against the addition of that element from the surface bulk. This results in a system of N_e redundant equations each containing the gas blowing rate, $\dot{m}$. At convergence, the correct blowing rate uniquely fulfills every elemental balance equation, making them numerically redundant. As noted by Bianchi, et al.[17], any of the elemental diffusion equations may be used to determine the mass blowing rate since the surface composition is fixed by the free-energy minimization process.

With the finite-rate surface chemistry module, surface energy balance including bulk phase enthalpy was also considered in solving for the surface temperature. It can easily be considered here, though, for simplicity, the sample calculations were run with purely radiative equilibrium since the objective was only to test the equilibrium solver and the interfacing numerics of the tools rather than obtain accurate wall temperatures to match a particular physical situation.

IV. Example Problem

A. Spherical Capsule

A test of the integration between the "black-box" equilibrium saturated mixture solver and the DPLR CFD code[18] was developed consisting of a spherical capsule with a 2.5-m shoulder-to-shoulder radius and freestream conditions of U=5.0 km/s, T=270 K, and ρ=0.001 kg/m^3. The surface was considered to be a source of bulk carbon C(b) only. Eight gaseous chemical species are considered – CO_2, CO, N_2, O_2, NO, C, N, and O – with air composed of N_2 and O_2 as present in the freestream. The surface is considered to be in radiative equilibrium with an emissivity of ε=0.89. The heat shield is modeled at zero angle of attack as an axially symmetric geometry.

The "black-box" interface between the codes was designed as an iterative process in which an explicit update to the composition and blowing rate is made at user-specified intervals. Some number of updates is required for the CFD solution to (hopefully) reach a steady state, but the number and frequency of those updates was not known at the start of this exercise. One philosophy is to let the CFD code fully converge to machine zero or at least to an acceptable tolerance level before applying each update from the equilibrium saturated mixture solver. However, it is not obvious that this is a necessary requirement. At the other extreme, the update procedure can be called every iteration to update concentration and mass flow rate. Without implicit Jacobian information, this can cause stability

issues if the wall temperature is fluctuating too rapidly and the mass flow rate or concentration changes are drastic enough. In such a case, under-relaxation is needed; in this case, however, it was found that the problem converged fine without any relaxation, providing some confidence that such an approach may not be needed for many problems.

The mass flow rate changes at the stagnation point and the associated convergence of residual, as measured by the L_2-norm of the global continuity equation, are plotted for four cases in Fig. 5. In these cases, the saturated equilibrium mixture update was made every 1 iteration (Fig. 5(a)), every 100 iterations (Fig. 5(b)), every 250 iterations (Fig. 5(c)), and every 1000 iterations (Fig. 5(d)). The baseline non-catalytic flowfield fully converges in about 1000 iterations, so this last case is indicative of the extreme of letting the flowfield fully converge between successive boundary condition updates. For clarity, a symbol is shown on the mass flow rate line for each plot at the iterations where an update is made. For the cases with longer intervals between updates, a sudden jump in residual is obvious each time the boundary is updated, creating a "saw-tooth" pattern in the residual history. The case where the boundary condition is updated every iteration never shows this behavior because the flow evolves with the boundary condition simultaneously, but the mass flow rate does go through significantly larger oscillations than observed with the longer interval cases.

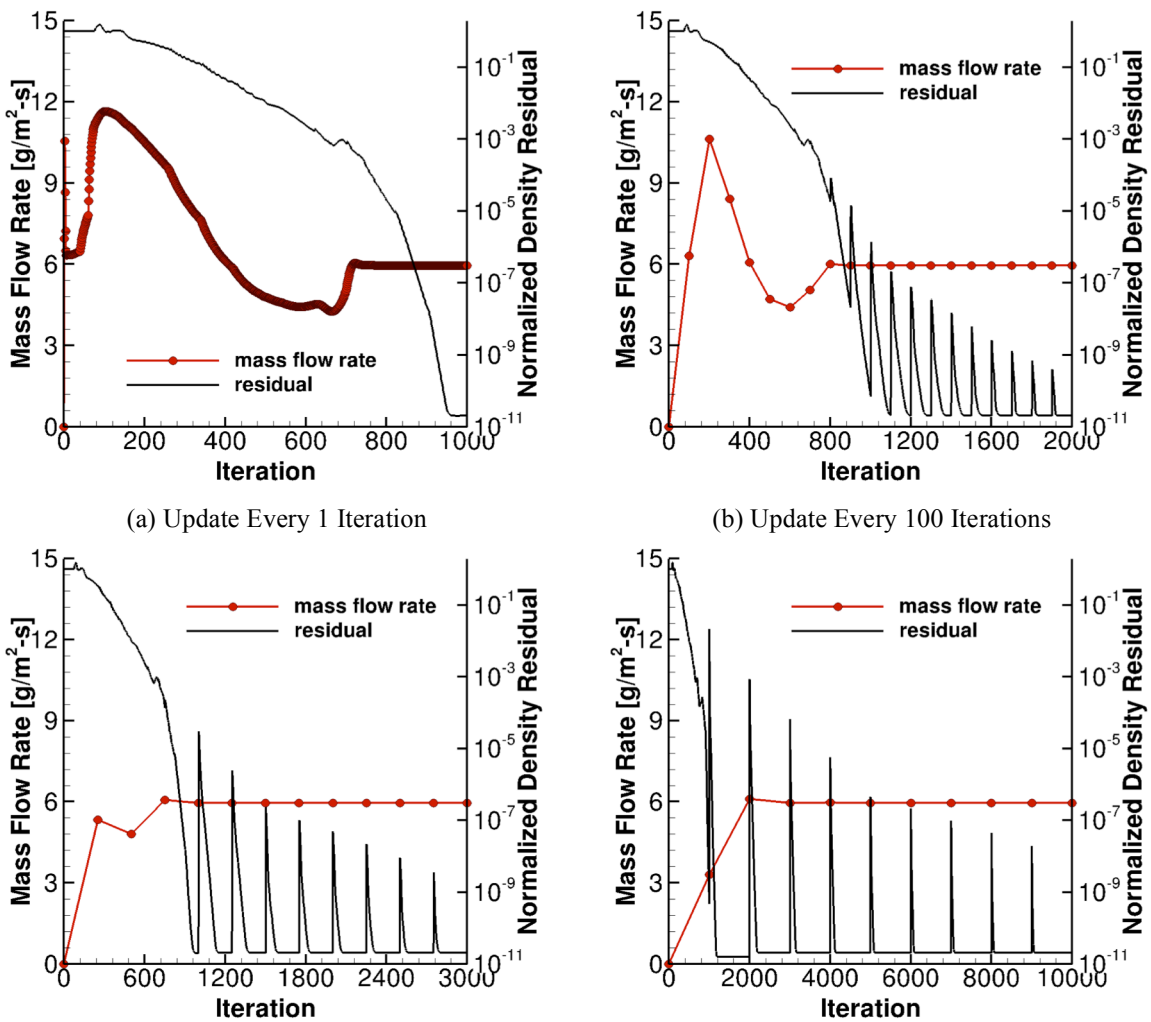

(a) Update Every 1 Iteration

(b) Update Every 100 Iterations

(c) Update Every 250 Iterations

(d) Update Every 1000 Iterations

Figure 5. Surface Mass Flow Rate and Residual (log scale) Convergence Histories for CFD Solution Coupled to Equilibrium Saturated Mixture Composition

The convergence of mass flow rate is the main metric by which this process must be judged. This is re-plotted for all four cases in Fig. 6. In Fig. 6(a), the mass flow rate at the stagnation point is plotted for the four update

scenarios as a function of the number of updates made to the boundaries. The results plotted in this way are very misleading since they suggest that the iteration1000 case reaches mass flow convergence in the fewest number of updates (this is a true statement), but it must be noted that the CFD solution is fully-converged in between each of these updates. At this same index of updates, the iteration1 case has barely advanced the CFD solution at all. However, for a well-converged flowfield, the mass flow rate has converged to within 1% of its final value after the third update and to within four significant digits of accuracy by the fifth update. Thus, we can confirm the statement by Olynick, et al.[4] that they obtained sufficient accuracy after three iterations despite the fact that their approach utilized the heat/mass transfer equivalency assumption of Eqn. (2).

When the convergence of the mass flux for the four cases is instead plotted versus iteration number, the effort expended for each of the solutions is clearer. It is apparent from this comparison that optimum convergence rate of the CFD and external solver (saturated equilibrium mixture in this case) is not obtained. It seems from these results that it is indeed more efficient to update the boundary conditions periodically in the evolution of the CFD flowfield. In fact, convergence of the mass balance of the solver is obtained for the iteration1, iteration100, and iteration250 cases after about the same number of iterations. This suggests that periodic updates are a better technique than

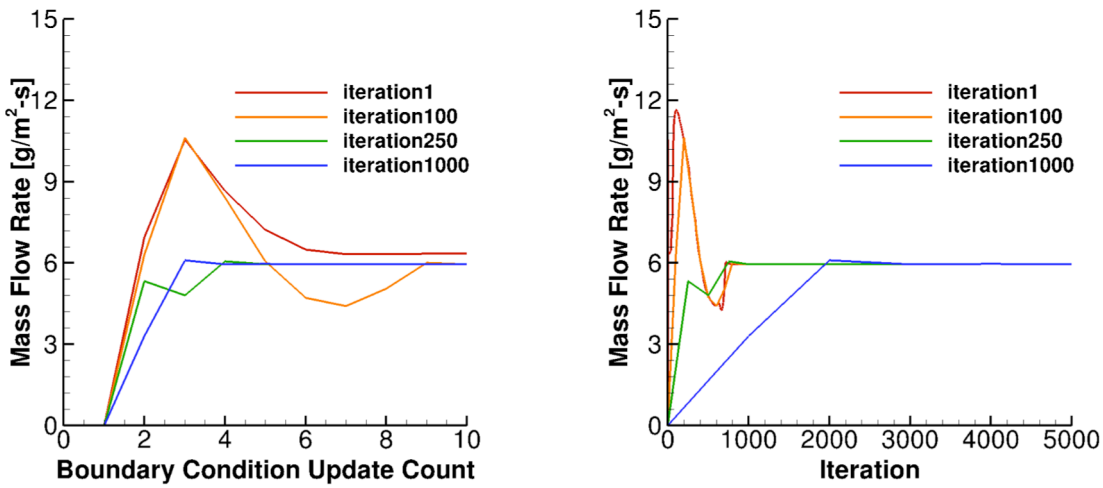

(a) vs. Update Count (b) vs. Iteration Number

Figure 6. Stagnation Point Mass Blowing Rate Convergence Behavior for Spherical Capsule Test Case

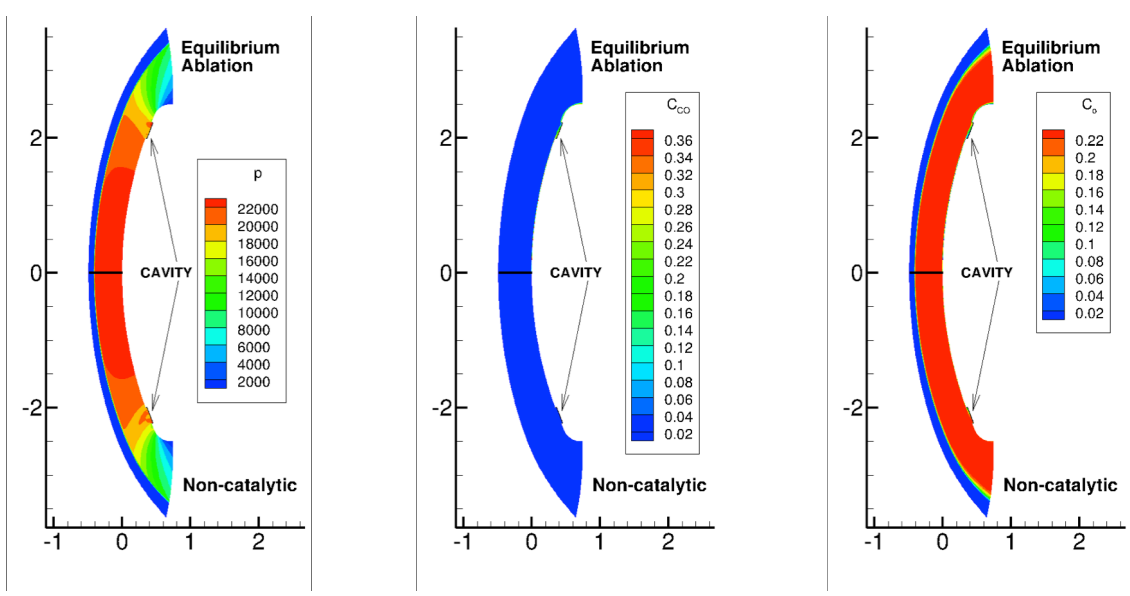

(a) Pressure (b) CO Mass Fraction (c) O Mass Fraction

Figure 7. Field Contours for Spherical Capsule with Heat Shield Cavity

letting the CFD solver converge fully each time. It is also emphasized that Fig. 6 shows that the same final mass flow rate at the stagnation point is eventually obtained regardless of the intervals of updating. It was unclear at the outset of this effort if there was a possibility that an unconverged flowfield/boundary condition state could be obtained that was dependent on the user defined selections, but this result inspires confidence that a unique solution can be obtained.

B. Spherical Capsule with Cavity

A second test case was briefly considered which consisted of the same spherical capsule with a 2.5-m shoulder-to-shoulder radius and freestream conditions of U=5.0 km/s, T=270 K, and r=0.001 kg/m^3. As before, eight chemical species are considered – CO_2, CO, N_2, O_2, NO, C, N, and O – with air composed of N_2 and O_2 are present in the freestream and a surface composed of carbon bulk, C(b). The surface is considered to be in radiative equilibrium with an emissivity of ε=0.89. The heat shield is modeled at zero angle of attack as an axially symmetric geometry. Just inside the shoulder of the heat shield, a cavity is placed which represents a simplified compression pad. In this simplified, axisymmetric grid, the cavity is a revolved channel or groove in the heat shield, but the physical processes entrained by the cavity should be qualitatively similar to a three-dimensional compression pad.

The pressure field, and mass fraction of species CO and O are shown in Fig. 7. In each case, the solution with a non-catalytic surface is shown in the lower part of each image and the equilibrium ablation solution is shown in the upper part of each image. Although the pressure fields are very similar, the equilibrium ablation boundary condition clearly results in the consumption of atomic oxygen in the near wall region of the boundary layer and the corresponding production of carbon monoxide. A closer view of the equilibrium ablation cavity is shown in Fig. 8. A number of near-wall streamlines are super-imposed on the image showing the complex interaction of the cavity. This interaction pattern will be dependent on cavity geometry, shock layer conditions and laminar/turbulent flow regimes among other things, but the pattern of interaction is reasonable in appearance. It is clear that the cavity is largely filled with a significant amount of carbon monoxide, impacting the ablation pattern of such a cavity on the heat shield. The surface temperature profile and the

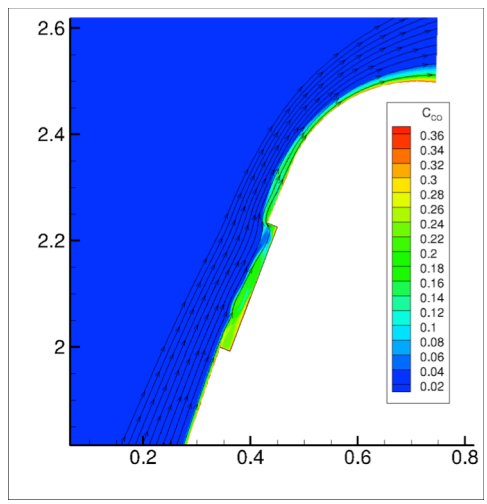

Figure 8. Cavity Region Carbon Monoxide Mass Fraction

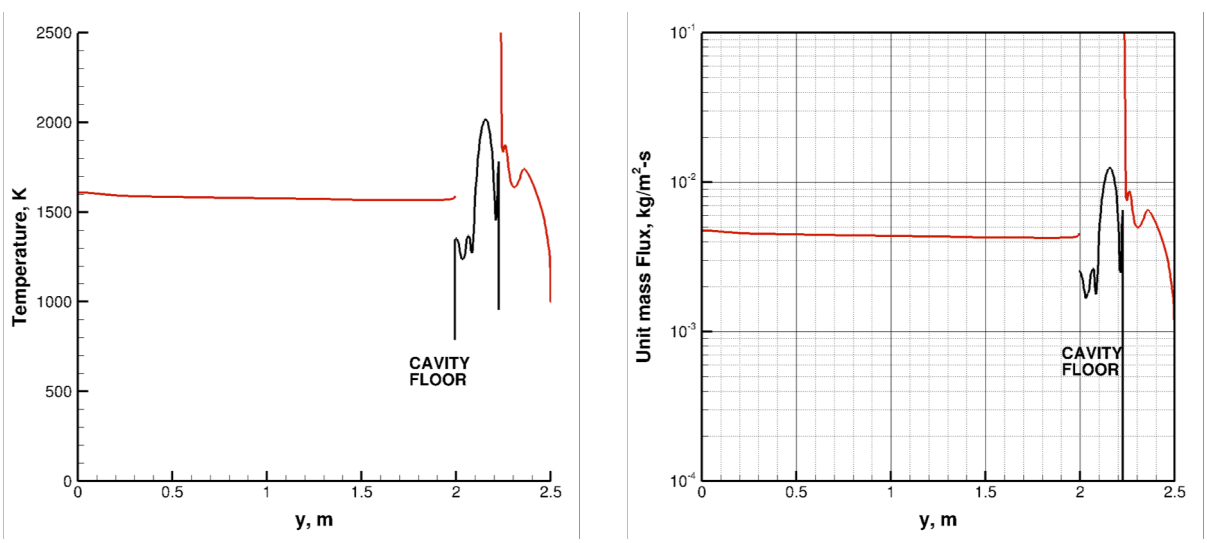

(a) Surface Temperature (b) Unit Blowing Rate [log scale]

Figure 9. Surface Temperature and Blowing Rate Contours for Spherical Capsule with Heat Shield Cavity

surface blowing rate profile are plotted in Fig. 9. In each case, the profile along the bottom of the cavity is shown as indicated. The sidewalls of the cavity are not included since they occur at a nearly constant y value and contribute nothing to the plot. Here, the complex interaction of the cavity region again is apparent. The mass blowing rate and the corresponding surface temperature changes dramatically across the cavity floor, increasing near the aft end where the external flow streamlines penetrate the cavity. In this case, laminar flow has been assumed, but the possibility of transition in the cavity shear layer will clearly impact the profile in and downstream of the cavity.

V. Conclusions

A generalized equilibrium saturated mixture solver was developed based on the CEA algorithm which determines the equilibrium composition of a mixture of constituents including the presence of gas, liquid, or solid materials. This algorithm has been employed to determine the equilibrium saturation of a mixture of gases to a bulk source of elemental material as a function of temperature and pressure. This generalized approach may be used to generate blowing rate (B') curves for complex bulk systems consisting of multiple surface constituents and multiple elementals. This approach extends a classic approach that limits equilibrium saturation from one source at a time. This solver was used to generate B' curves for a complex material mimicking the properties of AVCOAT char.

This tool was used to explore the coupling of a material response solver to a common hypersonic CFD code to develop a capability for coupled ablation solution. This coupling was intentionally done explicitly by treating the equilibrium saturated mixture solver as a "black-box" where Jacobian information was not available to the CFD linear solver. Preliminary tests indicated that the explicit coupling is possible for realistic cases and that the optimum boundary condition update frequency should be performed at intervals where the CFD solution is in an intermediate state rather than waiting for full convergence to update the boundary each time. The selection of the update frequency was fairly insensitive to the convergence of the combined boundary conditions for choices between updating each iteration and updating after full convergence. In practice, the analysis suggests it would be possible to update the boundary conditions at intervals directed by reaching a certain threshold of convergence rather than a specified number of iterations, but optimization was not a major concern of the exercise.

Acknowledgments

This project was sponsored by grant #NNX10AP41G from NASA Johnson Space Center, technical monitor Brian P. Anderson.

References

[1]Martin, A. and Boyd, I. "Strongly Coupled Computation of Material Response and Nonequilibrium Flow for Hypersonic Ablation," AIAA Paper 2009 – 3597. 41ST AIAA Thermophysics Conference, San Antonio, TX: 22 – 25 June 2009.

[2]Nompelis, I.; Candler, G.; and Conti, R. "A Parallel Implicit CFD Code for the Simulation of Ablating Re-Entry Vehicles," AIAA Paper #2009 – 1562. 47TH AIAA Aerospace Sciences Meeting, Orlando, FL: 5 – 8 January 2009.

[3]Milos, F. and Rasky, D. "Review of Numerical Procedures for Computational Surface Thermochemistry," *Journal of Thermophysics and Heat Transfer*, Vol. 8, No. 1, January – March 1994, Pgs. 24 – 34.

[4]Olynick, D.; Chen, Y.-K.; and Tauber, M. "Aerothermodynamics of the Stardust Sample Return Capsule," *Journal of Spacecraft and Rockets*, Vol. 36, No. 3, May – June 1999, Pgs. 442 – 462.

[5]Johnston, C.; Gnoffo,P.; and Mazaheri, A. "Study of Ablation-Flowfield Coupling Relevant to the Orion Heat Shield," *Journal of Thermophysics and Heat Transfer*, Vol. 26, No. 2, 2012, Pgs. 213 – 221.

[6]Marschall, J. and MacLean, M. "Finite-Rate Surface Chemistry Model, I: Formulation and Reaction System Examples" AIAA Paper 2011–3783. 42ND Thermophysics Conference, Honolulu, HI: 27 – 30 June 2011.

[7]MacLean, M.; Marschall, J.; and Driver, D. "Finite-Rate Surface Chemistry Model, II: Coupling to Viscous Navier-Stokes Code" AIAA Paper 2011–3784. 42ND Thermophysics Conference, Honolulu, HI: 27 – 30 June 2011.

[8]Bianchi, D.; Nasuti, F.; and Martelli, E. "Navier-Stokes Simulations of Hypersonic Flows with Coupled Graphite Ablation," *Journal of Spacecraft and Rockets*, Vol. 47, No. 4, July – August 2010, Pgs. 554 – 562.

[9]Gordon S. and McBride, B. "Computer Program for Calculation of Complex Chemical Equilibrium Compositions and Applications," NASA–RP–1311. October 1994.

[10]McBride, B.; Zehe, M.; and Gordon, S. "NASA Glenn Coefficients for Calculating Thermodynamic Properties of Individual Species," NASA/TP–2002–211556. September 2002.

[11]Blackwell, B.F. and Howard, M.A. "An Element Potential Based Chemical Equilibrium Solver for Gas/Surface Thermochemistry," AIAA Paper 2012 – 0815. Jan. 2012.

[12]Candler, G. "Nonequilibrium Processes in Hypervelocity Flows: An Analysis of Carbon Ablation Models," AIAA 2012–0724. Jan. 2012.

[13]Graves, R.A. and Witte, W.G. "Flight-Test Analysis of Apollo Heat-Shield Material using the Pacemaker Vehicle System," NASA TN D-4713. August 1968.

[14]Bartlett, E.P., Anderson, L.W., and Curry, D.M. "An Evaluation of Ablation Mechanisms for the Apollo Heat Shield Material," *J. Spacecraft*, Vol. 8, No. 5, May 1971, Pgs. 463 – 469.

[15]Milos, F.S. and Marschall, J. "Thermochemical Ablation Model for TPS Materials with Multiple Surface Constituents," AIAA 1994 – 2042.

[16]Milos, F.S. and Chen, Y.-K. "Comprehensive Model for Multicomponent Ablation Thermochemistry," AIAA Paper 97 – 0141. Jan 1997.

[17]Bianchi, D.; Martelli, E.; and Onofri, M. "Practical Navier-Stokes Computation of Flowfields with Ablation Products Injection," Thermal Protection Systems and Hot Structures, Proceedings of the 5th European Workshop held 17-19 May, 2006 at ESTEC, Noordwijk, The Netherlands. Edited by K. Fletcher. ESA SP-631. European Space Agency, 2006. Published on CDROM, p.15.1.

[18]Wright, M.J.; Bose, D.; and Candler, G.V. "A Data Parallel Line Relaxation Method for the Navier-Stokes Equations". *AIAA Journal*. Vol 36, no 9. Pgs 1603 – 1609. Sept 1998.